

# Atomic bubbles in impurity-stabilized solid $^4\text{He}$

V. Lebedev, P. Moroshkin, and A. Weis

*Physics Department, University of Fribourg, Chemin du Musée 3, 1700 Fribourg, Switzerland*  
E-mail: victor.lebedev@unifr.ch

Received January 4, 2009

The optical absorption and fluorescence spectra of alkali atoms isolated in liquid and solid He matrices depend on specific macroscopic matrix properties, such as their molar volume and (anisotropic) elasticity constants, and provide thus information about the quantum matrix. We have applied optical spectroscopy to investigate the properties of a recently discovered impurity-stabilized doped  $^4\text{He}$  solid that exists in equilibrium with pressurized superfluid helium close to the solidification/melting point of pure helium. The difference between the local He density around the implanted atoms obtained in the present experiment and the average density measured earlier suggests that the impurity-stabilized solid He is in fact a porous structure filled with liquid helium.

PACS: 61.72.-y Defects and impurities in crystals; microstructure;  
61.72.S- Impurities in crystals.

Keywords: absorption spectra, optical spectroscopy, superfluid helium, solid helium.

## Introduction

In a recent publication [1] we have described a new phenomenon taking place during the melting of solid helium doped with alkali (Rb or Cs) atoms and clusters. The doped part of the helium crystal melts at a lower pressure than pure He and remains solid even when the rest of the pure helium sample is completely molten. We call this solid structure standing in liquid He an iceberg. Using an interferometric technique we have shown [1] that the helium density of the iceberg lies in between those of solid and liquid helium. It was also shown in Ref. 1 that alkali atoms implanted into the He crystal mostly aggregate into clusters with a characteristic diameter of 20–80 nm. The number density of those clusters is  $10^9$ – $10^{10}$   $\text{cm}^{-3}$ . Besides that, the sample contains  $10^8$ – $10^9$  neutral alkali atoms per  $\text{cm}^3$  that are trapped in the crystal as individual objects [2] (atomic bubbles) and positive alkali ions and free electrons at a density of  $10^{14}$ – $10^{15}$   $\text{cm}^{-3}$  [3].

The interaction between neutral alkali-metal particles and He atoms is strongly repulsive because of the Pauli principle that forbids any overlap between the closed electronic shell of the He atom and the valence electrons of the alkali atoms. On the other hand, an inhomogeneous electric field around a positive ion can polarize and attract He atoms — an effect known as electrostriction. In liquid helium it results in the formation of a solid helium shell around the positive ion, a structure called snowball.

Snowballs of positive alkali ions in liquid He have been observed in Ref. 4. According to our hypothesis suggested in Ref. 1, the helium atoms in the iceberg are bound by the electrostriction effect produced by positive alkali ions distributed in the sample.

The optical absorption and fluorescence spectra of alkali atoms isolated in liquid and solid  $^4\text{He}$  matrices are described with high accuracy by the atomic bubble model [5,6]. The spectra depend on specific macroscopic matrix properties, such as its molar volume and (anisotropic) elasticity constants, and provide thus information about the quantum matrix. In the present paper we apply optical spectroscopy to investigate the properties of alkali dopants in the impurity-stabilized solid He iceberg.

## Atomic bubbles

The atomic bubble model for metal atoms embedded into liquid and solid helium has been developed in Refs. 5–7. An atomic bubble is a microscopic cavity formed around an impurity atom in condensed helium because of the strong repulsive interaction (Pauli repulsion) between the valence electron of the impurity atom and the closed electronic shells of the He atoms. The shape and the size of the bubble can be found by minimizing the total energy of the atom plus bubble system composed of the Cs–He interaction term,  $U_{\text{Cs-He}}$ , the pressure-volume

work,  $pV_{\text{bubble}}$ , the surface energy,  $\sigma S$ , the volume kinetic energy due to the localization of He atoms at the bubble interface leading to a distortion of the density  $\rho$ , and the energy  $U_{\text{elast}}$ , due to the elastic strain in the matrix. The last term appears only for the solid helium matrices:

$$E_{\text{tot}} = U_{\text{Cs-He}} + pV_{\text{bubble}} + \sigma S + \frac{h}{16\pi m_{\text{He}}} \int d^3R \frac{(\nabla \rho)^2}{\rho} + U_{\text{elast}}. \quad (1)$$

Both electronic states of the Cs atom involved in a resonant optical transition have spherically symmetric orbitals. The interaction energy  $U_{\text{Cs-He}}$  has been calculated in Refs. 5, 6 using a pseudopotential approach. Absorption and fluorescence spectra calculated assuming a spherical bubble shape, are found to be in very good agreement with experimental results in liquid and bcc solid helium. For the uniaxial hcp crystal the anisotropy of the elastic properties has to be taken into account in the last term of Eq. (1). This results in a slightly deformed bubble [8]. In the case of barium, the upper  $6P_1$  state has a nonspherical orbital. In the calculations reported in Refs. 9, 10 the interaction energy was computed using *ab initio* Ba-He pair potentials. The resulting theoretical spectra overestimate the blueshift by several nanometers.

### Experiment

#### Experimental setup

The sample is prepared in three steps: solidification of pure  $^4\text{He}$ , doping the  $^4\text{He}$  crystal with Cs or Ba, and then melting the pure solid He surrounding the doped part of the crystal. The experimental setup is described in detail in Ref. 11. The helium crystal is grown in a copper cell with an inner volume of  $170 \text{ cm}^3$  by applying pressure from an external He reservoir. The cell is immersed in superfluid  $^4\text{He}$  cooled to 1.5 K by pumping on its surface.

The doping is usually performed at a temperature of 1.5 K and a helium pressure of 29–30 bar (region A in Fig. 1). Cs or Ba atoms are implanted into the crystal by means of laser ablation with a pulsed frequency doubled Nd:YAG laser focused from above onto a solid metallic target at the bottom of the cell. The heat deposited by the laser melts a part of the crystal above the target and the ablated atoms, ions, and clusters diffuse into the liquid helium. By moving the focusing lens (inside the superfluid helium bath) upwards, we create inside of the solid He a vertical channel filled with liquid He, a few millimeters in diameter and about 2–3 cm in height. When the laser is switched off, liquid helium filling the channel solidifies and impurity particles become trapped in the crystal. In the last step we slowly release helium from the cell via a needle-valve until the crystal starts to melt. As we have described in Ref. 1, the melting proceeds from the top of

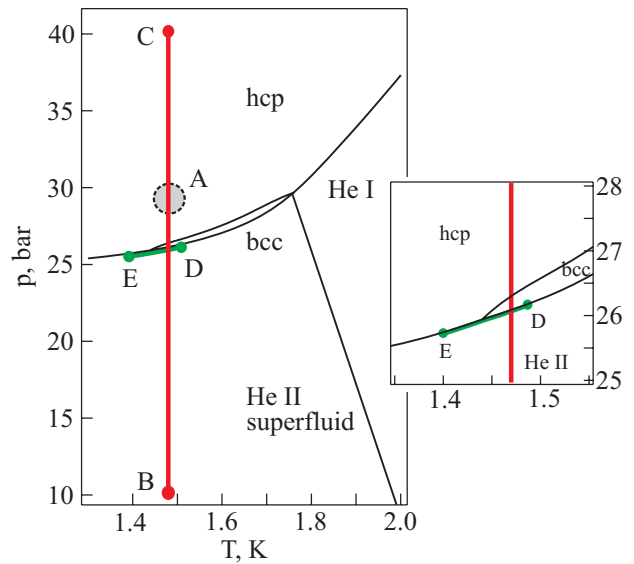


Fig. 1. Phase diagram of condensed  $^4\text{He}$ : A marks the conditions of the implantation; the measurements discussed in the paper were made along the lines BC and ED.

the cell to the bottom. Via the lateral windows of the cryostat and the pressure cell we observe the liquid–solid interface moving downwards. The doped part of the crystal having approximately the same shape as the molten channel during the doping process now stays solid and is surrounded by liquid He. We stop the release of He pressure when the liquid–solid interface drops below the cell windows. The experiments described in the present paper were performed with such a sample, with the temperature and pressure varied along the melting curve of pure  $^4\text{He}$ . The results are compared with those obtained in bulk solid He.

Metal atoms implanted in the iceberg are excited by the (pulsed) radiation of a tunable optical parametric oscillator (OPO) pumped by a third harmonic of a pulsed Nd:YAG laser. For the Cs-doped samples we use the idler output of the OPO for exciting the  $6S_{1/2}-6P_{1/2}$  transition at 850 nm (894 nm in the free Cs atom). For the Ba-doped samples the signal output of the OPO is used. In the latter case we excite the  $6S_0-6P_1$  transition at 540 nm (553.5 nm in the free Ba atom). The laser-induced fluorescence is collected at right angle and analyzed by a grating spectrograph equipped with a CCD camera.

#### Experiments with Cs

A typical laser-induced fluorescence spectrum from the iceberg doped with Cs atoms is shown in Fig. 2, a. In the same Figure we show spectra obtained with the same sample before melting: in bulk hcp solid He at 27 bar (just above the hcp to bcc transition) and in bulk bcc solid He at 26.6 bar (just above the melting point). All three spectra are strongly broadened and blueshifted with respect to the

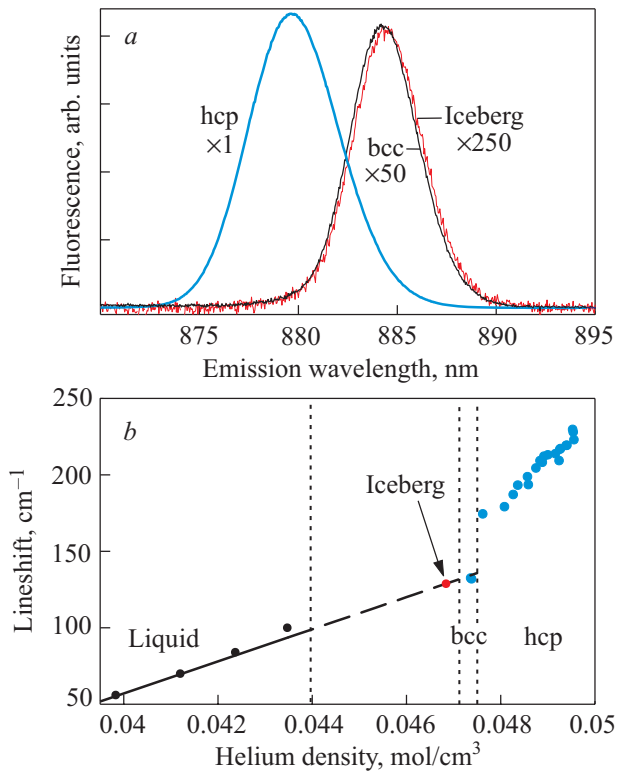


Fig. 2. (a) Laser-induced fluorescence spectra from Cs-doped bulk bcc and hcp solid  $^4\text{He}$  and from the iceberg. (b) Shift of the fluorescence spectrum as a function of He molar density at 1.5 K (along the line BC in Fig. 1). The data for bulk liquid and bulk solid He are taken from Refs. 5 and 6, respectively.

free Cs atom. One can see that the spectrum in the iceberg is very close to that in the bulk bcc solid. At the same time the spectra in the two crystalline phases of solid He can be easily distinguished. In Fig. 2, b the spectral shift of the transition is plotted as a function of the He molar density  $\rho$  at a constant temperature of the sample (along the line BC in Fig. 1). The range of densities corresponds to the helium pressure varying from 10 to 40 bar. The data for bulk liquid and bulk solid He are taken from Refs. 5 and 6, respectively. In general, the blueshift is proportional to the increase of the density (i.e., of the He pressure). This behavior is very well reproduced by the spherical bubble model [5,6]. The transition from the liquid phase into bcc solid is accompanied by a density increase of approximately 8%. If one extrapolates the linear dependence obtained in Ref. 5 for pressurized liquid He, one finds a transition wavelength in bcc solid in agreement with our observations. The sudden jump of the transition wavelength at the bcc to hcp phase boundary is due to the sudden change of the elastic properties of the crystal: the hcp crystal is stiffer and possesses a different type of anisotropy. The shift of the spectral line can be explained if one considers nonspherical atomic bubbles. Figure 2 shows that the wavelength of the laser-induced fluorescence is a good measure of the He density and allows us to distin-

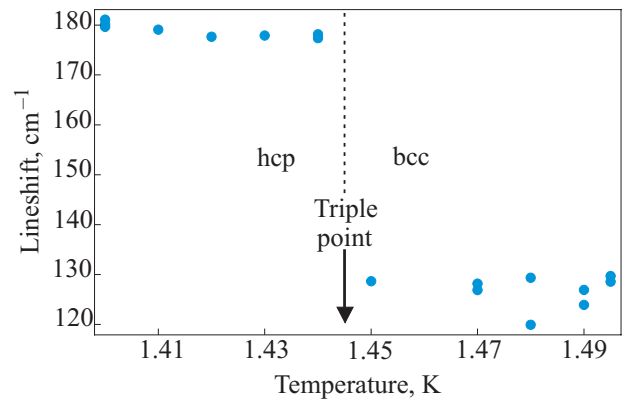


Fig. 3. Shift of the laser-induced fluorescence spectrum in a Cs-doped iceberg as a function of the sample temperature (along the line ED in Fig. 1).

guish between the two crystalline phases, although the density difference between them is very small (about 1%). Another conclusion that can be drawn from Fig. 2 is that the crystalline structure of the iceberg is most likely bcc and its density is very close to that in a bulk bcc crystal.

In order to check whether the crystalline structure of the iceberg is always bcc or whether it corresponds to the structure of bulk pure  $^4\text{He}$  under the same pressure and temperature, we have varied the temperature of the sample, moving along the melting line in the phase diagram of pure  $^4\text{He}$  (line DE in Fig. 1). The results of this experiment are shown in Fig. 3. Here one can see a clear jump of the transition frequency at a temperature of 1.45 K, that corresponds to the lower triple point of pure  $^4\text{He}$ , where the solid phase in equilibrium with liquid changes its structure from bcc to hcp. The magnitude of the jump in the iceberg (Fig. 3) is identical to that in bulk solid  $^4\text{He}$  (Fig. 2, a). This leads us to conclude that doped solid He in the iceberg undergoes a bcc to hcp phase transitions under the same conditions as the pure bulk  $^4\text{He}$  does.

#### Experiments with Ba

Solid He samples doped with barium behave very similarly than the Cs-doped samples. The increased stability of Ba-doped solid helium against melting has been reported for the first time in Ref. 12 and the spectra of the  $6S_0-6P_1$  transition of Ba in liquid and solid He were studied in Refs. 9, 10, 12. We have remeasured the fluorescence spectrum of Ba atoms in bulk solid He and for the first time obtained a Ba spectrum in an iceberg standing in liquid He. The fluorescence spectra obtained in bulk bcc  $^4\text{He}$ , bulk hcp  $^4\text{He}$  and in the iceberg at 1.5 K are shown in Fig. 4, a and the density dependence of the spectral shift is plotted in Fig. 4, b (the data in bulk liquid He are taken from Ref. 12). One can see that the density dependence has the same character as in the Cs-doped sample, but the

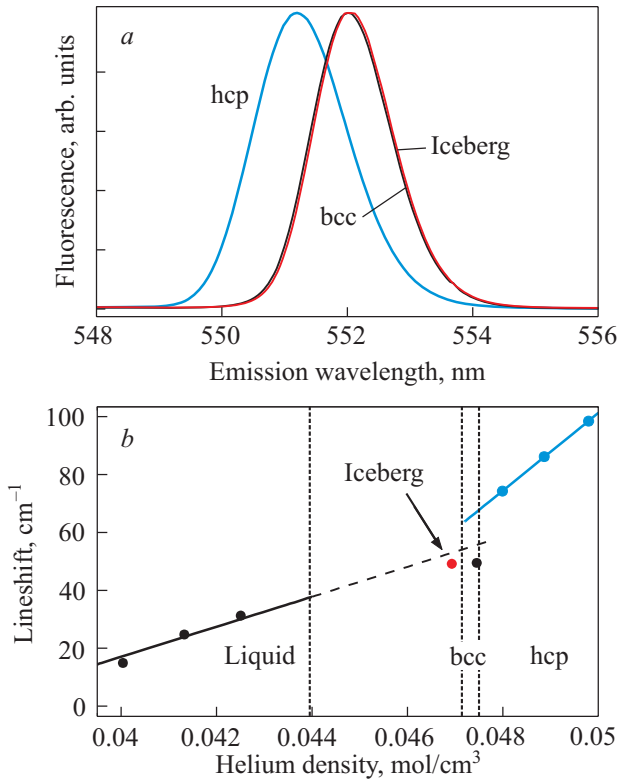


Fig. 4. (a) Laser-induced fluorescence spectra from Ba-doped bulk bcc and hcp solid  $^4\text{He}$  and from the iceberg. (b) Shift of the fluorescence spectrum as a function of He molar density at 1.5 K (along the line BC in Fig. 1). The data for bulk liquid He are taken from Ref. 12.

magnitude of the spectral shift and broadening is about two times smaller. The spectrum obtained in the iceberg is almost indistinguishable from that in the bulk bcc  $^4\text{He}$  crystal.

The results of the experiment with Ba show that the mechanism of the iceberg formation is not specific for alkali-metal atoms and can be realized with alkali-earth elements as well. Moreover, we have found that the clusterization of implanted Ba atoms proceeds much slower than in the case of Cs and that the resulting number density of atomic Ba bubbles in bulk solid He and in the Ba-doped iceberg is several orders of magnitude higher.

### Discussion

The results of the present study show that the iceberg consists of doped He crystals whose properties (crystalline structure, density) do not differ from those of pure solid He. Note that the He density inferred from these spectroscopic experiments is the *local density* around the impurity atoms. On the other hand, an interferometric experiment [1], sensitive to the *average density* of the iceberg, suggests that the density is significantly smaller than that of pure solid He, but larger than the density of pressurized liquid He close to the solidification point. It

seems that it contains both doped solid He and undoped liquid He. We therefore suggest that the iceberg is a porous, doped solid structure filled with liquid He.

The impurity atoms in liquid He quickly form metallic clusters and cannot be excited by the laser resonant with the atomic transition. In experiments with liquid He significant concentrations of implanted atoms could be maintained only by using a very high repetition rate of the ablation laser, or by applying a second sputtering laser [5,13]. No such cluster dissociation laser pulses were applied in the present experiment. Therefore, the Cs and Ba atoms situated inside the pores of the iceberg filled with liquid He did not contribute to the observed fluorescence spectrum. This explains also the very low intensity of the fluorescence from the Cs-doped iceberg as compared to the fluorescence in bulk solid He (note the normalization factors in Fig. 2,a).

A filling factor, defined as  $V_{\text{solid}}/V_{\text{total}}$ , can be determined from the average density  $\rho_{\text{iceberg}}$  measured in Ref. 1:

$$\rho_{\text{iceberg}} = \frac{V_{\text{solid}}}{V_{\text{total}}} \rho_{\text{solid}} + \left(1 - \frac{V_{\text{solid}}}{V_{\text{total}}}\right) \rho_{\text{liquid}}. \quad (2)$$

With  $\rho_{\text{iceberg}} \approx \rho_{\text{liquid}} + 0.25(\rho_{\text{solid}} - \rho_{\text{liquid}})$  [1] we obtain  $V_{\text{solid}}/V_{\text{total}} \approx 0.25$ . According to the hypothesis suggested in Ref. 1, the stability of the iceberg is due to the high concentration of positive ions. The ionic number density in Cs and Rb-doped iceberg obtained in Ref. 3 is  $N_i \approx 10^{14} - 10^{15} \text{ cm}^{-3}$ . Assuming that the ions are concentrated in the solid part of the iceberg, we obtain a local ionic density  $N_{\text{loc}}$  that is four times larger. The average distance between neighboring ions is thus  $d \approx N_{\text{loc}}^{-3} \approx 62 - 120 \text{ nm}$ . This is still significantly larger than the distance at which He atoms in liquid He become bound to the ion (i.e., a snowball radius), measured in Ref. 4 to be 0.84 nm. It should also be noted that, according to Ref. 14, the singly-charged alkaline-earth ions should form bubbles rather than the snowballs. However, in our experiments the Ba-doped samples behave very similarly than the alkali-doped ones. More experimental and theoretical studies are needed in order to clarify the mechanism of the iceberg formation. A challenging project would be the recording of magnetic resonance spectra of alkali atoms in the iceberg. It was shown [8] that those spectra are extremely sensitive to the local crystalline structure.

### Summary

We have studied the properties of the recently discovered impurity-stabilized solid  $^4\text{He}$  (iceberg) by means of laser spectroscopy of embedded metallic (Cs, Ba) atoms. We have shown that the local density of  $^4\text{He}$  in the iceberg is very close to that of bulk solid  $^4\text{He}$ . On the other

hand, the average density of iceberg, measured in Ref. 1 lies in between those of bulk liquid and bulk solid He. We suggest that the iceberg is in fact a porous solid structure filled with liquid He and estimate the volume of the solid fraction to be 0.25 of the total iceberg volume.

1. P. Moroshkin, A. Hofer, S. Ulzega, and A. Weis, *Nature Physics* **3**, 786 (2007).
2. M. Arndt, R. Dziewior, S. Kanorsky, A. Weis, and T.W. Hänsch, *Z. Phys.* **B98**, 377 (1995).
3. P. Moroshkin, V. Lebedev, and A. Weis, *to be published*.
4. W.I. Glaberson and W.W. Johnson, *J. Low Temp. Phys.* **20**, 313 (1975).
5. T. Kinoshita, K. Fukuda, Y. Takahashi, and T. Yabuzaki, *Phys. Rev.* **A52**, 2707 (1995).
6. A. Hofer, P. Moroshkin, S. Ulzega, D. Nettels, R. Müller-Siebert, and A. Weis, *Phys. Rev.* **A76**, 022502 (2007).
7. M. Beau, H. Günther, G. zu Putlitz, and B. Tabbert, *Z. Phys.* **B101**, 253 (1996).
8. S. Kanorsky, S. Lang, T. Eichler, K. Winkler, and A. Weis, *Phys. Rev. Lett.* **81**, 401 (1998).
9. S. Kanorsky, A. Weis, M. Arndt, R. Dziewior, and T. Hänsch, *Z. Phys.* **B98**, 371 (1995).
10. H. Bauer, M. Beau, B. Friedl, C. Marchand, K. Miltner, and H.J. Reyher, *Phys. Lett.* **A146**, 134 (1990).
11. P. Moroshkin, A. Hofer, S. Ulzega, and A. Weis, *Fiz. Nizk. Temp.* **32**, 1297 (2006) [*Low Temp. Phys.* **32**, 981 (2006)].
12. M. Arndt, *Ph.D Thesis*, Ludwig Maximilians Universität München, Max-Planck-Institut für Quantenoptik, Garching, MPQ-Report 197 (1995).
13. A. Fujisaki, K. Sano, T. Kinoshita, Y. Takahashi, and T. Yabuzaki, *Phys. Rev. Lett.* **71**, 1039 (1993).
14. M.W. Cole and R.A. Bachman, *Phys. Rev.* **B15**, 1388 (1977).